

# Quantitative aspects of the dynamical impurity approach

Krunoslav Požgajčić\*

*Universität des Saarlandes, Institut für Theoretische Physik*

*Saarbrücken, Germany*

(Dated: February 2, 2008)

A calculation technique in the context of the self-energy functional approach (SFA) and its local form, the dynamical impurity approach (DIA)<sup>1</sup>, will be proposed. This technique allows for a precise calculation of the derivatives of the grand potential functional used in the search for a stationary point. To make a closer comparison of the DIA with the dynamical mean-field theory (DMFT)<sup>2</sup>, and to demonstrate the proposed technique, we calculated paramagnetic U-T phase diagram of the Hubbard model at half-filling, which exhibits metal-insulator transition.

PACS numbers: 71.15.-m, 71.30.+h

## I. INTRODUCTION

Variational determination of the grand potential functional has a long history. The seminal paper, made in the 1960s<sup>3</sup>, provides us with the expression for the grand potential functional which reads

$$\Omega[\mathbf{G}] = \Phi[\mathbf{G}] + \text{Tr} \ln(-\mathbf{G}) - \text{Tr}((\mathbf{G}_0^{-1} - \mathbf{G}^{-1})\mathbf{G}), \quad (1)$$

where  $\mathbf{G}_0$  is the free Green's function,  $\mathbf{G}$  is the full Green's function and  $\Phi[\mathbf{G}]$  is the Luttinger-Ward functional expressed by a sum over all connected skeleton diagrams.  $\Omega[\mathbf{G}]$  is stationary for the physical Green's function  $\mathbf{G}$ . The main problem which arises in that approach is a formidable skeleton perturbation expansion. Approaches which used Eq. (1) as a starting point would approximate the Luttinger-Ward functional by an incomplete diagram series or by composing  $\Phi[\mathbf{G}]$  from only a few lowest order diagrams<sup>4</sup>. Recently it has been proposed to regard the grand potential functional as a functional of the self-energy with the Legendre transform of the Luttinger-Ward functional calculated from a simplified Hamiltonian (which we will refer to as a reference system) and the self-energy of the original system approximated by the one of the reference system<sup>1</sup>. Mathematically expressed, the proposal states that

$$\begin{aligned} \Omega_t[\Sigma(t')] &= \Omega_{t'}[\Sigma(t')] + \text{Tr} \ln(-(\mathbf{G}_0^{-1} - \Sigma(t'))^{-1}) \\ &\quad - \text{Tr} \ln(-(\mathbf{G}'_0{}^{-1} - \Sigma(t'))^{-1}), \end{aligned} \quad (2)$$

where  $\Sigma[t']$  is the exact self-energy of the reference system,  $\mathbf{G}'_0$  is the free Green's function of the same and  $\mathbf{G}_0$  is the free Green's function of the original system. The reference Hamiltonian is chosen such that it is simpler than the original one, while a systematic increase in its size would reproduce the original system. In the case of the Hubbard model<sup>5,6,7</sup>, correlated sites in the reference system correspond to those from the original one. We can add uncorrelated sites to correlated sites to mimic the rest of the lattice<sup>1,8</sup>. The grand potential functional is stationary with respect to the variation of the exact self-energy. The same stationarity condition will be imposed to the approximate one defined by Eq. (2) with

the reference system being simpler than the original one. The simplest form of the reference system is obtained if we restrict our attention to the local self-energy, in which case we speak of the dynamical impurity approach (DIA). In general, including reference systems with non-local self-energies, the method is called self-energy functional approach. In this account we will concentrate on the calculation performed in the context of DIA, even though, only slight changes are necessary for a more general, SFA approach.

In the seminal paper<sup>1</sup> it was demonstrated on the example of the Mott-Hubbard transition how even a rudimentary reference system can give a good account of the physics obtained by the numerically more expensive DMFT approach. We are going to address the question of how the extension of the reference system improves the results. Since DIA is equivalent to DMFT only when the number of uncorrelated sites goes to infinity, it will be interesting to compare the convergence of the results obtained in DIA to those obtained in DMFT as the number of uncorrelated sites in the reference system is increased. Contrary to the mentioned rudimentary case with only one variational variable, the set of variational parameters in the reference system with six atoms has five components for the half-filled case. To be able to determine borders of the phase diagram precisely, we calculate derivatives of the grand potential functional analytically. This procedure will be sketched in Section II together with additional calculations given in the appendices. In the Section III we present the results for the Hubbard model.

## II. DETERMINATION OF THE STATIONARY POINT

The main numerical burden of the SFA/DIA method is the determination of the self-energy. That part consists of the diagonalization of the reference system, calculation of the Green's function from the Lehmann representation and, using Dyson's equation, determination of the self-energy. The only numerically problematic part is the one of the calculation of the self-energy from the Green's function (see Appendix B). With the obtained

self-energy we can evaluate trace terms along the lines already discussed in some earlier accounts<sup>8</sup>. That approach would demand numerical calculation of derivatives for the determination of the stationary points of the grand potential functional. The numerical load for a reliable and precise calculation of derivatives can be large<sup>9</sup>. We will show how the additional information from the diagonalized reference system can be used for their determination. The biggest advantage of the method can be seen in the coexistence region of the phase diagram.

Before embarking on the calculation of derivatives of the trace terms, we are going to sketch a few steps in the calculation of the trace terms already discussed<sup>8</sup>. Using a general form of the Green's function  $\mathbf{G}$ , the trace term can be written as

$$\text{Tr} \ln(-\mathbf{G}) = \sum_{\omega_n} \frac{e^{i\omega_n 0^+}}{\beta} \text{tr} \ln \frac{-1}{i\omega_n + \mu - \mathbf{t} - \Sigma(i\omega_n)}, \quad (3)$$

where  $\text{tr}$  denotes trace over all quantum states. A function of a Hermitian operator is defined as  $f(A) = Uf(a)U^\dagger$  where  $a$  is the diagonalized  $A$  matrix and  $U$  is the unitary transformation which performs it. If  $\eta_k(i\omega_n)$  are eigenvalues of the operator  $\mathbf{t} + \Sigma(i\omega_n)$ , then

$$\text{Tr} \ln(-\mathbf{G}) = \sum_{\omega_n} \sum_k \frac{e^{i\omega_n 0^+}}{\beta} \ln \frac{-1}{i\omega_n + \mu - \eta_k(i\omega_n)}. \quad (4)$$

Summation over  $k$  encompasses all eigensolutions of the operator  $\mathbf{t} + \Sigma(i\omega)$ . In order to get over from the summation over Matsubara frequencies to the integration in the complex plane, a standard trick is applied. It consists in the introduction of a function in the complex plane which has poles at  $z = i\omega_n$  and the subsequent integration around the contour which includes the imaginary axis

$$\text{Tr} \ln(-\mathbf{G}) = \sum_k \oint_C \frac{-dz}{2\pi i} \frac{e^{z0^+}}{e^{\beta z} + 1} \ln \frac{-1}{z + \mu - \eta_k(z)}. \quad (5)$$

The integration contour in Eq. (5) can be mapped to the integration contour enclosing the real axis by the lines infinitesimally above and below it ( $\omega \pm i\delta$ ). Using analytic properties of the integrand, i.e.,  $\eta_k(\omega - i\delta) = \eta_k^*(\omega + i\delta)$ , and retaining only the largest contributions in  $0^+$  and  $\delta$  (both are infinitesimally small positive numbers), we can express  $\text{Tr} \ln(-\mathbf{G})$  as

$$\sum_k \int_{-\infty}^{\infty} \frac{-d\omega}{\pi} f(\omega) \text{Im} \ln \frac{-1}{\omega + i0^+ + \mu - \eta_k(\omega + i0^+)}, \quad (6)$$

where  $f(\omega) = 1/(e^{\beta\omega} + 1)$  is the Fermi-Dirac function. For a function  $F(\omega + i0^+)$  that has the property  $\text{Im} F(\omega + i0^+) \leq 0$  (that is the case for the diagonal Green's function), there follows the equality  $\text{Im} \ln(-F(\omega + i0^+)) = \pi \Theta(F(\omega)) = \pi \Theta(1/F(\omega))$ , with  $\Theta$  being the step function. Due to the finite number of poles in the reference system, singular points don't give a finite contribution to the integral. The resulting expression for the trace term reads

$$\text{Tr} \ln(-\mathbf{G}) = - \sum_k \int_{-\infty}^{\infty} d\omega f(\omega) \Theta(\omega + \mu - \eta_k(\omega)). \quad (7)$$

This expression is our starting point for calculating derivatives with respect to the parameters of the reference system. As in the calculation of the grand potential functional<sup>8</sup>, we want to obtain the integrand as a sum of the Dirac  $\delta$ -functions, which is then trivially integrated. For this purpose we just have to exchange integration over the real axis and derivative with respect to the reference system parameter  $\lambda$ . Due to the discontinuity of the argument of the step function in Eq. (7), we obtain two sums of the  $\delta$ -functions, one evaluated in the zeros of  $\omega + \mu - \eta_k(\Sigma(\mathbf{t}'), \omega)$  and the other evaluated in the poles of  $\eta_k(\Sigma(\mathbf{t}'), \omega)$ .

$$\frac{\partial}{\partial \lambda} \text{Tr} \ln(-\mathbf{G}[\Sigma(\mathbf{t}')]) = - \frac{\partial}{\partial \lambda} \sum_k \int_{-\infty}^{\infty} d\omega f(\omega) \Theta(\omega + \mu - \eta_k(\Sigma(\mathbf{t}'), \omega)) \quad (8)$$

$$= \sum_k \int_{-\infty}^{\infty} d\omega f(\omega) \left[ \delta(\omega + \mu - \eta_k(\omega)) \frac{\partial \eta_k(\Sigma(\mathbf{t}'), \omega)}{\partial \lambda} - \delta\left(\frac{1}{\omega + \mu - \eta_k(\Sigma(\mathbf{t}'), \omega)}\right) \frac{\partial \frac{1}{\omega + \mu - \eta_k(\Sigma(\mathbf{t}'), \omega)}}{\partial \lambda} \right] \quad (9)$$

$$= \sum_{k,i} f(\omega_{i,k}^{(z)}) \frac{\partial \eta_k(\Sigma(\mathbf{t}'), \omega_{i,k}^{(z)})}{\partial \lambda} \frac{1}{\left|1 - \frac{\partial \eta_k(\Sigma(\mathbf{t}'), \omega)}{\partial \omega}\right|_{\omega=\omega_{i,k}^{(z)}}} - \sum_{k,j} f(\omega_{j,k}^{(p)}) \frac{\partial \eta_k(\Sigma(\mathbf{t}'), \omega_{j,k}^{(p)})}{\partial \lambda} \frac{1}{\left|1 - \frac{\partial \eta_k(\Sigma(\mathbf{t}'), \omega)}{\partial \omega}\right|_{\omega=\omega_{j,k}^{(p)}}}. \quad (10)$$

The second term in Eq. (10) should be thought of as an evaluation of the derivatives for  $\omega \rightarrow \omega_{j,k}^{(p)}$ , since each of the derivatives diverges for  $\omega = \omega_{j,k}^{(p)}$ . Using the notation

---


$$\frac{\partial}{\partial t_i} \text{Tr} \ln(-G[\Sigma(\mathbf{t}')]]) = - \sum_{k,j} f(\omega_{j,k}^{(p)}) \frac{\langle \Psi_{k,j} | \mathbf{C}_j^{(2),d\Sigma} | \Psi_{k,j} \rangle}{\langle \Psi_{k,j} | \mathbf{C}_j^{(1),\Sigma} | \Psi_{k,j} \rangle} + \sum_{k,i} f(\omega_{i,k}^{(z)}) \frac{\partial \eta_k(\Sigma(\mathbf{t}'), \omega_{i,k}^{(z)})}{\partial t_i} \frac{1}{\left| 1 - \frac{\partial \eta_k(\Sigma(\mathbf{t}'), \omega)}{\partial \omega} \right|_{\omega=\omega_{i,k}^{(z)}}}}, \quad (11)$$


---

where  $|\Psi_{k,j}\rangle$  is an eigenstate of the matrix  $\mathbf{C}_j^{(1),\Sigma}$ . Equation (11) is completely general, i.e., it can also be applied to the case of non-local self-energy. From now on, we are going to apply it only to the case of the local self-energy.

For obtaining the grand potential functional we have to evaluate two trace terms: one for the Green's function of the original system and one for the Green's function of the reference system [see Eq. (1)]. Reference systems with the local self-energy can have any form (chainlike, starlike etc.), because reference systems with different configuration of bath sites can be mapped to each other so that the physical Green's function doesn't change. We have chosen the star-like reference system for its simplicity, with the Hamiltonian given as (the paramagnetic state is assumed)

$$H^{SIAM} = \sum_{\sigma} (\epsilon_c - \mu) c_{\sigma}^{\dagger} c_{\sigma} + U n_{\uparrow} n_{\downarrow} + \sum_{l,\sigma} (\epsilon_{a,l} - \mu) a_{l,\sigma}^{\dagger} a_{l,\sigma} + \sum_{l,\sigma} V_l (c_{l,\sigma}^{\dagger} a_{l,\sigma} + a_{l,\sigma}^{\dagger} c_{l,\sigma}). \quad (12)$$

The trace of the full Green's function of the reference system can be decomposed in a number of trace terms with the scalar Green's functions

$$\begin{aligned} \text{tr}' \ln(-\mathbf{G}'(i\omega)) \\ = \sum_{\sigma} \ln(-G'_{1,\sigma}(i\omega)) + \sum_{\sigma} \sum_{k=2}^{N_a} \ln(-G'_{k,\sigma}(i\omega)), \end{aligned} \quad (13)$$

with  $G'_k(i\omega_n) = 1/(i\omega_n + \mu - \epsilon_k)$  and

$$G'_1(i\omega_n) = \frac{1}{i\omega_n + \mu - \epsilon_1 - \sum_{k=2}^{N_a} \frac{V_k^2}{i\omega_n + \mu - \epsilon_k} - \Sigma(i\omega_n)} \quad (14)$$

Using the notation of Eq. (10), the following identifications can be done:

$$\eta_1(i\omega_n) = \epsilon_1 + \sum_{k=2}^{N_a} \frac{V_k^2}{i\omega_n + \mu - \epsilon_k} + \Sigma(i\omega_n) \quad (15)$$

$$\eta_{k>1} = \epsilon_k \quad (16)$$

The original Green's function is diagonalized by the Fourier transformation under assumption of the local

of Eqs. (B13, B14), but with coefficients being matrices instead of scalars, we can obtain the final expression for the derivative of the trace term. It reads

self-energy and translation invariance of the system. In this case  $\eta_{k,\sigma}(\omega) = \epsilon(k) + \Sigma(\omega)$ , where  $\epsilon(k)$  is the Fourier transformed one-particle term and  $k$  denotes a wave number.

Stationary point in the parameter space  $\mathbf{t}'$  assures us that we have found the self-energy which is physical. Since it is possible to find more than one solution, thermodynamically stable are only those characterized by the minimum of the grand potential<sup>8</sup>.

### III. METAL-INSULATOR TRANSITION IN THE HUBBARD MODEL

As a demonstration of the above numerical procedure, we determined the U-T phase diagram of the Hubbard model in the paramagnetic state. In addition to the results for two-site DIA which have shown qualitative agreement with the full DMFT calculations, we will demonstrate that richer reference systems allow us to make quantitative comparisons with the existing DMFT calculations<sup>10,11,12</sup>.

In contrast to the DMFT, where the local Green's function of the reference system is identified with the one of the original system, we have to distinguish the two in the DIA formalism. The difference between DMFT and DIA procedures is best seen from the stationarity condition of the grand potential functional which results in the identity

$$\sum_{\omega_n} \sum_{n,m} \left[ \frac{1}{\mathbf{G}_0^{-1} - \Sigma(\mathbf{t}')} - \mathbf{G}' \right]_{mn} \left( \frac{\partial \Sigma(\mathbf{t}')}{\partial \lambda} \right)_{nm} = 0. \quad (17)$$

The self-energy in DIA is local ( $\Sigma_{n,m} = \delta_{n,m} \Sigma_n$ ). This implies that the stationarity is automatically fulfilled if the Green's function of the impurity site in the reference system is identical to the local Green's function of the original system. The identity of the two Green's functions in DIA formalism is expected only when the number of additional bath sites is large. In general, the local Green's function of the original system and the impurity Green's function of the reference system are related to each other by the self-energy which they share, but otherwise they are different. Thus to satisfy the stationarity

condition we also have to take into account the derivative of the self-energy with respect to a parameter of the reference system appearing in Eq. (17). In order to facilitate the search for a stationary point, we reduced the parameter space using particle-hole transformation which is a symmetry transformation of the Hubbard model at half-filling. This transformation is defined by the iden-

TABLE I: Constraints on the parameters of the reference system imposed by the particle-hole symmetry at half-filling ( $\epsilon_1 \equiv \epsilon_c, \epsilon_{l \geq 2} \equiv \epsilon_{a,l}$ ).  $N$  is the size of the reference system.

N	Variables and their relations
2	a) $V_2$
3	a) $V_2, V_3, \epsilon_2 = \epsilon_3 = \mu$ b) $V_3 = V_2, \epsilon_3 = 2\mu - \epsilon_2$
4	a) $V_2, V_3, V_4, \epsilon_2 = \epsilon_3 = \epsilon_4 = \mu$ b) $V_2, V_4 = V_3, \epsilon_4 = 2\mu - \epsilon_3, \epsilon_2 = \mu$
5	a) $V_2, V_3, V_4, V_5, \epsilon_2 = \epsilon_3 = \epsilon_4 = \epsilon_5 = \mu$ b) $V_2, V_3, V_5 = V_4, \epsilon_2 = \epsilon_3 = \mu, \epsilon_5 = 2\mu - \epsilon_4$ c) $V_3 = V_2, V_5 = V_4, \epsilon_3 = 2\mu - \epsilon_2, \epsilon_5 = 2\mu - \epsilon_4$
6	a) $V_2, V_3, V_4, V_5, V_6, \epsilon_2 = \epsilon_3 = \epsilon_4 = \epsilon_5 = \epsilon_6 = \mu$ b) $V_2, V_3, V_4, V_6 = V_5, \epsilon_2 = \epsilon_3 = \epsilon_4 = \mu, \epsilon_6 = 2\mu - \epsilon_5$ c) $V_2, V_4 = V_3, V_6 = V_5, \epsilon_2 = \mu, \epsilon_4 = 2\mu - \epsilon_3, \epsilon_6 = 2\mu - \epsilon_5$

tity  $Pc_{i,\sigma}P^{-1} = e^{i\phi_j}c_{i,\sigma}^\dagger$ , where  $\phi_i$ 's are chosen such that  $\phi_i - \phi_j = \pi$  and  $i, j$  are site indices. We can choose  $\phi = 0$  on the sites with even Manhattan distance and  $\phi = \pi$  for the remaining sites. The same transformation is performed on the impurity site. For the bath sites we have chosen such a particle-hole transformation that the resulting number of variational parameters is maximal. For the case of the impurity site with  $\phi = 0$ , bath sites should be transformed according to the expression  $Pa_{i,\sigma}P^{-1} = -a_{i,\sigma}^\dagger$ . The transformed  $H^{SIAM}$  Hamiltonian is then

$$\begin{aligned}
PHP^{-1} &= \sum_{\sigma} (\mu - \epsilon_c - U)c_{\sigma}^\dagger c_{\sigma} + U n_{\uparrow} n_{\downarrow} \\
&+ 2 \sum_l (\epsilon_l - \mu) + U + 2(\epsilon_c - \mu) + \sum_{l,\sigma} (\mu - \epsilon_{a,l}) a_{l,\sigma}^\dagger a_{l,\sigma} \\
&+ \sum_{l,\sigma} V_l (c_{l,\sigma}^\dagger a_{l,\sigma} + a_{l,\sigma}^\dagger c_{l,\sigma}).
\end{aligned} \quad (18)$$

Under the condition that the transformed Hamiltonian and the original Hamiltonian of the single impurity Anderson model (SIAM) are the same<sup>13</sup>, we can put constraints on the parameters of the reference system. Since  $\mu = U/2$ , we find immediately that  $\epsilon_c = 0$ . Bath states transform according to the equations:

$$\mu - \epsilon_{a,l} = \epsilon_{a,l'} - \mu, \quad V_l = V_{l'}. \quad (19)$$

Combinations following from Eq. (19) are listed in Table I for different sizes of the reference system. It can be shown that the effective size of the reference system is determined by the number of different  $\epsilon$ 's, on-site energies of the bath orbitals. Namely, for the orbitals with  $\epsilon$ 's equal to the chemical potential it is possible to perform

a unitary transformation that transforms uncorrelated sites with  $\epsilon_i = \mu$  into one site coupled to the impurity site and the rest of the uncorrelated sites uncoupled from the impurity site. For example, if we had two uncorrelated sites in the reference system with  $\epsilon_{2/3} = \mu$  then it can be shown that the Hamiltonian can be mapped to the one with the hopping amplitudes  $\tilde{V}_2 = \sqrt{V_2^2 + V_3^2}$ ,  $\tilde{V}_3 = 0$ . Thus the effective reference system has been reduced to a system with only one site. In the case of more bath sites with  $\epsilon_i = \mu$  we can iterate the transformation for two sites and show that the resulting effective amplitude is  $\tilde{V}_2 = \sqrt{\sum_{i=2}^N V_i^2}$ ,  $\tilde{V}_{i>2} = 0$ . The solutions in this work correspond to the cases 2a, 4b and 6c from Table I evaluated for the semicircular free-particle density of states. In Fig. (1) we show the calculated quasi-particle

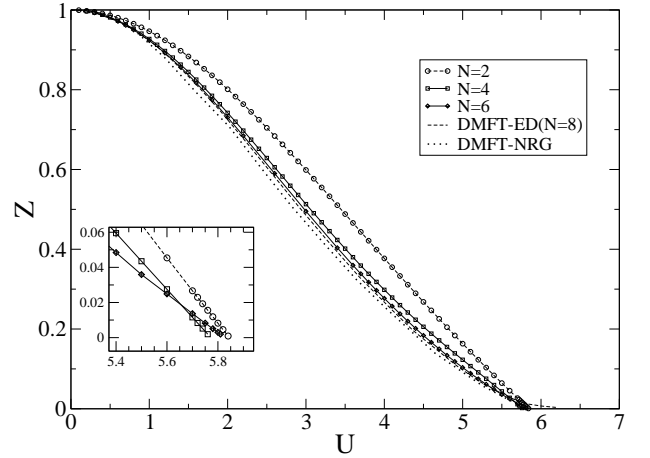


FIG. 1: Quasi-particle weight at  $T=0$  calculated in DIA for different sizes of the reference system ( $N=2,4,6$ ). Curves for ( $N=2,4$ ) have already been presented<sup>1</sup>. For comparison, DMFT results obtained using numerical renormalization group(NRG)<sup>14</sup> and exact diagonalization(ED)<sup>1</sup> as impurity solvers are included.

weight  $Z = 1/(1 - \partial \text{Re}\Sigma(\omega + i0^+)/\partial \omega)|_{\omega=0}$ . Regarding the interval of  $U$  values as a whole we can notice that the convergence of  $Z$  with increasing system size is uniform. That is not true in the vicinity of the phase transition. Even though the convergence is not uniform in that region, it seems to be fast. The comparison with DMFT calculation using exact diagonalization as impurity solver shows a close connection of the two methods. The phase diagram of the paramagnetic state of the Hubbard model in the  $U$ - $T$  plane is shown in Fig. (2). Three different regions in temperatures below the critical point, denoted by an empty circle, can be distinguished: (a) metallic phase for small values of  $U$ , (b) insulating phase for large  $U$ , (c) coexistence of both phases in a triangle-like shape for the intermediate Coulomb interaction. Whereas the transition below the critical point is of the first order, we find the crossover from the metallic to the insulating solution in temperatures above the critical point. Convergence of the phase diagram for different sizes of the reference sys-

tem is shown in the inset of Fig. (2). On the metallic side

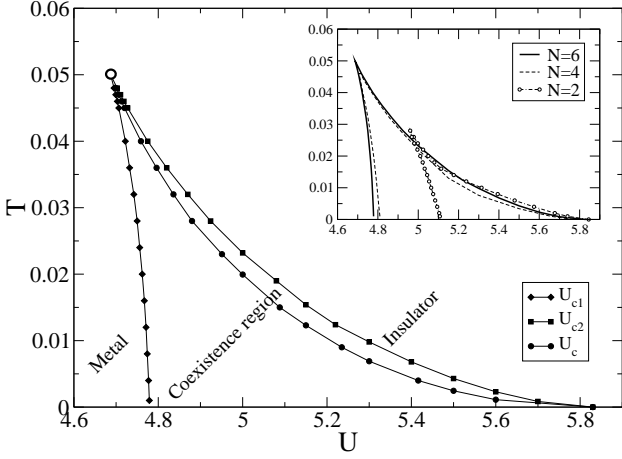


FIG. 2: U-T phase diagram of the paramagnetic state of the Hubbard model.  $U_{c1}$  curve denotes the left border of the region with the insulating solution.  $U_{c2}$  is the right border of the region with the metallic solution. Coexistence region has both solutions. The insulating solution is stable to the right of the curve  $U_c$ , whereas the metallic solution is stable on its left. The empty circle indicates the critical point separating low and high temperature regions with the first and the second order phase transitions between metallic and insulating solution respectively.  $U_{c1}$  and  $U_{c2}$  curves for different sizes of the reference system ( $N=2,4,6$ ) are shown in the inset.

of the metal-insulator transition in the DMFT formalism, the central role is played by a three peak structure in the spectral function, the middle peak corresponding to the Abrikosov-Suhl resonance in the impurity model and two Hubbard bands. That distribution of the spectral weight together with Table I can explain the convergence trends in the solutions found for different sizes of the reference system. For  $N = 2$  we have only one pole in the inverse of the free Green's function of the reference system at the Fermi level. From the DMFT equation for the semi-circular density of states  $G_{0,\sigma}^{-1}(\omega_n) = i\omega_n + \mu - t^2 G_\sigma(\omega_n)$  it would follow that the local Green's function has only one pole on the Fermi level if the equation holds for each number of bath sites. In the DIA formalism the connection between the on-site Green's function and the inverse of the free Green's function in the reference system of a finite size is more involved, but we believe that rapid convergence of the DIA results to those obtained in DMFT allows us to use the DMFT equation for the argumentation. This means that, with  $N=2$ , we cannot properly account for the Hubbard bands central to the insulating phase. The  $U_{c1}$  curve is thus substantially underestimating the extension of the insulating phase region in comparison with  $N = \{4,6\}$  results. The same reasoning explains why  $N = \{3,5\}$  reference systems show no improvement of the metallic solution with respect to the reference systems with a smaller but even number of sites. A reference system with an odd number of sites,

due to the particle-hole symmetry, has no pole in the inverse of the free Green's function at the Fermi level or it has two poles at the Fermi level which can be mapped to one. For  $N = 4$  we can account for the side bands, and

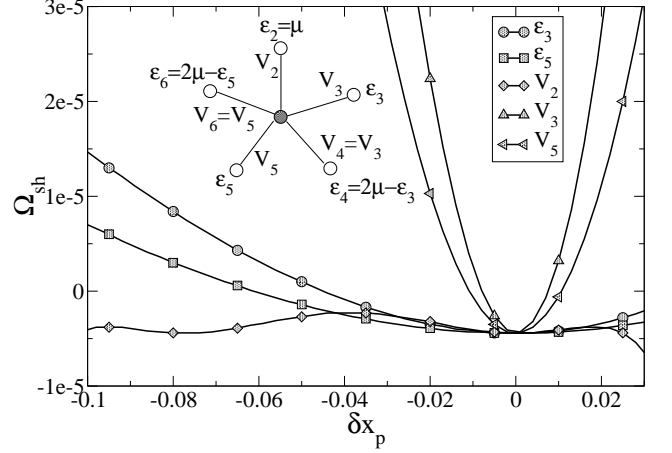


FIG. 3: Shifted grand potential functional in the direction of the parameters of the reference system around the insulating solution for  $T=0.016$  and  $U=4.77$ . Grand potential functional is given by  $\Omega = \Omega_{sh} + 2.50717$ . Schematic configuration of the reference system with the corresponding parameters is shown in the upper left corner.

$N = 6$  brings only a slight change to the phase diagram. Boundaries in the phase diagram are defined by the disappearance of a stationary point in the parameter space for either metallic or insulating solution. An example of the parameter space is shown in Fig. (3). The calculation was done for six atoms. At half-filling and in the paramagnetic state there are five independent parameters (upper left corner of the figure). The parameter space is shown in the region around the stationary point for the insulating phase and  $U=4.77$ ,  $T=0.016$ . Insulating solution disappears when the stationarity condition is not any more fulfilled in the direction  $V_2$ . As already argued,  $V_2$  is related to the weight of the Green's function of the original system at the Fermi level. Another comparison of the calculations done in the DMFT framework with the DIA calculation is shown in Fig. (4) for the whole phase diagram. As already noticed for  $T=0$ , the DIA calculation shows strong resemblance to the DMFT-ED results.

In conclusion, we showed how additional information from the reference system can be used to increase the precision of the calculation in the context of DIA. Comparisons with the results obtained in DMFT demonstrate close connection between the DIA and DMFT-ED procedures. The advantage of the DIA formulation over the DMFT-ED formulation is particularly clear for the case when the number of bath sites is not sufficiently large to reproduce the local Green's function of the original system<sup>1</sup>. Already for  $N = 6$ , DIA and DMFT-ED give almost the same result for the metal-insulator transition



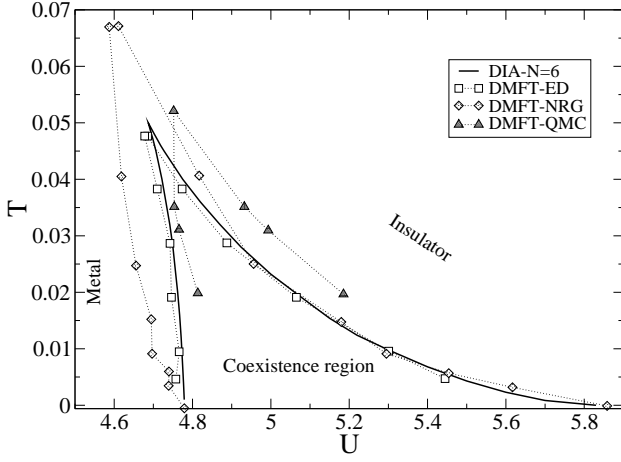


FIG. 4: Metal-insulator transition in the half-filled Hubbard model. The solid line shows the result from DIA with a reference system of the size  $N=6$ . DMFT results with ED(squares)<sup>10</sup>, NRG(diamonds)<sup>12</sup> and quantum Monte Carlo(triangles)<sup>11</sup> as impurity solver are shown for comparison.

in the paramagnetic state of the Hubbard model at half-filling.

I would like to thank Prof. C. Gros for his help in a part of this work, M. Potthoff for kindly providing additional information on the SFA prior to the publication, and W. Krauth for a stimulating discussion.

## APPENDIX A: DERIVATIVE OF THE GREEN'S FUNCTION

In Eq. (7) and all subsequent ones we evaluate the real part of the self-energy and the Green's function on the real axis (poles are excluded). Thus we will be interested only in the derivatives of the real parts of those functions. Since Green's functions are calculated from their Lehmann representation,

$$\text{Re}G_{ab}(\omega) = \frac{1}{N_d} \sum_{i=1}^{N_d} \sum_n \left[ \frac{\langle n|c_a^\dagger|n_g^{(i)}\rangle \langle n|c_b^\dagger|n_g^{(i)}\rangle}{\omega - (E_n - E_0)} + \frac{\langle n|c_b|n_g^{(i)}\rangle \langle n|c_a|n_g^{(i)}\rangle}{\omega - (E_0 - E_n)} \right], \quad (\text{A1})$$

where  $N_d$  is the degeneracy of the ground state,  $|n_g^{(i)}\rangle$  are degenerate ground-state eigenfunctions and  $E_0$  is the ground-state energy, the derivative with respect to  $\omega$  is straightforward to evaluate. Summation over  $n$  extends over all eigenstates. In Eq. (A1) we used the fact that the matrix representation of the Hamiltonian and the corresponding eigenfunctions will be real, and organized all matrix elements so that the ground states are in the ket state.

The derivative of the Green's function with respect to a parameter of the reference system  $\lambda \in \{\epsilon_i, V_i\}$  can be

calculated by applying the derivative to its Lehmann representation. For each pair of indices  $(i, n)$  there are two terms contributing to the Green's function, where the first term is the projection of the state created out of the  $N$ -particle ground state upon addition of a particle, on the eigenstates of the  $(N+1)$ -particle system. The second term is the projection of the ground state with added hole. We can get the second term by performing the following replacements in the first term:  $c_a^\dagger \Rightarrow c_a$ ,  $c_b^\dagger \Rightarrow c_b$ , and by exchanging energies ( $E_0 \Leftrightarrow E_n$ ) in the denominator. The derivative of the first term is

$$\begin{aligned} \frac{\partial}{\partial \lambda} \frac{\langle n|c_a^\dagger|n_g^{(i)}\rangle \langle n|c_b^\dagger|n_g^{(i)}\rangle}{\omega - (E_n - E_0)} &= \frac{\frac{\partial \langle n|c_a^\dagger|n_g^{(i)}\rangle}{\partial \lambda} \langle n|c_b^\dagger|n_g^{(i)}\rangle + \frac{\partial \langle n|c_b^\dagger|n_g^{(i)}\rangle}{\partial \lambda} \langle n|c_a^\dagger|n_g^{(i)}\rangle}{\omega - (E_n - E_0)} \\ &+ \frac{\langle n|c_a^\dagger|n_g^{(i)}\rangle \langle n|c_b^\dagger|n_g^{(i)}\rangle}{[\omega - (E_n - E_0)]^2} \left( \frac{\partial E_n}{\partial \lambda} - \frac{\partial E_0}{\partial \lambda} \right). \end{aligned} \quad (\text{A2})$$

In the term with  $\omega - (E_n - E_0)$  in the denominator, the second part in the numerator is obtained from the first by changing  $c_a^\dagger$  to  $c_b^\dagger$ . The remaining derivatives are:

$$\begin{aligned} \frac{\partial \langle n|c_a^\dagger|n_g^{(i)}\rangle}{\partial \lambda} &= \frac{\partial \langle n|}{\partial \lambda} c_a^\dagger |n_g^{(i)}\rangle + \langle n|c_a^\dagger \frac{\partial |n_g^{(i)}\rangle}{\partial \lambda}, \\ \frac{\partial E_n}{\partial \lambda} &, \quad \frac{\partial E_0}{\partial \lambda} \end{aligned} \quad (\text{A3})$$

In the end we have the problem of determining derivatives of eigenvectors and eigenvalues with respect to the parameter  $\lambda$ . It is well known that the terms up to the second order in the Rayleigh-Schrödinger perturbation theory correspond to the order of perturbation  $\lambda$ . We can thus use the perturbation to determine derivatives of eigenvalues and eigenvectors. Special attention should be paid to the case when some eigenstates are degenerate. If we denote the perturbation as  $H' = \lambda V$ , then, in the perturbation theory<sup>15</sup>, we have to use states from the subspace which diagonalize the operator  $V$ . Assuming that the above requirement is fulfilled, it follows that

$$\begin{aligned} \frac{\partial \langle n|c_a^\dagger|n_g^{(i)}\rangle}{\partial \lambda} &= \sum_{\substack{m \\ E_m \neq E_0}} \frac{\langle m|V|n_g^{(i)}\rangle \langle n|c_a^\dagger|m\rangle}{E_0 - E_m} \\ &+ \sum_{\substack{n' \\ E_{n'} \neq E_n}} \frac{\langle n'|c_a^\dagger|n_g^{(i)}\rangle \langle n'|V|n\rangle}{E_n - E_{n'}} \end{aligned} \quad (\text{A4})$$

and

$$\frac{\partial E_n}{\partial \lambda} = \langle n|V|n\rangle, \quad \frac{\partial E_0}{\partial \lambda} = \langle n_g^{(i)}|V|n_g^{(i)}\rangle \quad (\text{A5})$$

After some rearrangements, the derivative of the Green's

function has the form

$$\frac{\partial \text{Re}G_{ab}(\omega, \lambda)}{\partial \lambda} = \frac{1}{N_d} \sum_n \sum_{i=1}^{N_d} \left\{ \frac{A_{i,n}^{ab}}{\omega - (E_n - E_0)} + \frac{B_{i,n}^{ab}}{\omega - (E_0 - E_n)} + \frac{C_{i,n}^{ab}}{[\omega - (E_n - E_0)]^2} + \frac{D_{i,n}^{ab}}{[\omega - (E_0 - E_n)]^2} \right\}, \quad (\text{A6})$$

with weights of the first order poles given by

$$\begin{aligned} A_{i,n}^{ab} = & \sum_{\substack{n' \\ E_{n'} \neq E_n}} \frac{\langle n'|V|n \rangle}{E_n - E_{n'}} \left( \langle n'|c_a^\dagger|n_g^{(i)} \rangle \langle n|c_b^\dagger|n_g^{(i)} \rangle \right. \\ & + \langle n|c_a^\dagger|n_g^{(i)} \rangle \langle n'|c_b^\dagger|n_g^{(i)} \rangle \Big) \\ & + \sum_{\substack{m \\ E_m \neq E_0}} \frac{\langle m|V|n_g^{(i)} \rangle}{E_0 - E_m} \left( \langle n|c_a^\dagger|m \rangle \langle n|c_b^\dagger|n_g^{(i)} \rangle \right. \\ & + \langle n|c_a^\dagger|n_g^{(i)} \rangle \langle n|c_b^\dagger|m \rangle \Big) \end{aligned} \quad (\text{A7})$$

and  $B_{i,n}^{ab} = A_{i,n}^{ab}(c_a^\dagger \Leftrightarrow c_a, c_b^\dagger \Leftrightarrow c_b)$ , where  $\Leftrightarrow$  means the

exchange of the operators. The second order poles have the weights  $C_{i,n}^{ab}$  equal to

$$\langle n|c_a^\dagger|n_g^{(i)} \rangle \langle n|c_b^\dagger|n_g^{(i)} \rangle \left( \langle n|V|n \rangle - \langle n_g^{(i)}|V|n_g^{(i)} \rangle \right) \quad (\text{A8})$$

and  $D_{i,n}^{ab} = -C_{i,n}^{ab}(c_a^\dagger \Leftrightarrow c_a, c_b^\dagger \Leftrightarrow c_b)$ .

Along the same lines we can calculate the derivative of the Green's function for finite temperatures. For the Green's function  $\text{Re}G_{ab}(\omega)$  being given by the Lehmann representation

$$\sum_{n,n'} \frac{1}{Z} (e^{-\beta E_{n'}} + e^{-\beta E_n}) \frac{\langle n'|c_a|n \rangle \langle n|c_b^\dagger|n' \rangle}{\omega - (E_n - E_{n'})}, \quad (\text{A9})$$

the derivative  $\frac{\partial \text{Re}G_{ab}(\omega)}{\partial \lambda}$  is given by the function

$$\sum_{n,n'} \left[ \frac{A_{n,n'}^{ab}}{\omega - (E_n - E_{n'})} + \frac{B_{n,n'}^{ab}}{[\omega - (E_n - E_{n'})]^2} \right], \quad (\text{A10})$$

with  $A_{n,n'}^{ab}$  equal to

$$\begin{aligned} & \frac{e^{-\beta E_n} + e^{-\beta E_{n'}}}{Z} \left[ \sum_{\substack{l \\ E_l \neq E_n}} \frac{\langle l|V|n \rangle}{E_n - E_l} \left( \langle l|c_a^\dagger|n' \rangle \langle n|c_b^\dagger|n' \rangle + \langle n|c_a^\dagger|n' \rangle \langle l|c_b^\dagger|n' \rangle \right) + \sum_{\substack{m \\ E_m \neq E_{n'}}} \frac{\langle m|V|n' \rangle}{E_{n'} - E_m} \left( \langle n|c_a^\dagger|m \rangle \langle n|c_b^\dagger|n' \rangle \right. \right. \\ & \left. \left. + \langle n|c_a^\dagger|n' \rangle \langle n|c_b^\dagger|m \rangle \right) \right] - \frac{1}{Z} \left[ e^{-\beta E_n} \left( \beta \frac{\partial E_n}{\partial \lambda} + \frac{1}{Z} \frac{\partial Z}{\partial \lambda} \right) + e^{-\beta E_{n'}} \left( \beta \frac{\partial E_{n'}}{\partial \lambda} + \frac{1}{Z} \frac{\partial Z}{\partial \lambda} \right) \right] \langle n|c_a^\dagger|n' \rangle \langle n|c_b^\dagger|n' \rangle \end{aligned} \quad (\text{A11})$$

and

$$\begin{aligned} B_{n,n'}^{ab} = & \frac{1}{Z} (e^{-\beta E_n} + e^{-\beta E_{n'}}) \langle n|c_a^\dagger|n' \rangle \langle n|c_b^\dagger|n' \rangle \\ & \times (\langle n|V|n \rangle - \langle n'|V|n' \rangle). \end{aligned} \quad (\text{A12})$$

## APPENDIX B: SELF-ENERGY AND ITS DERIVATIVES

Self-energy  $\Sigma(\mathbf{t}', \omega)$  is defined by the Dyson equation

$$\Sigma(\omega) = \mathbf{G}_0^{-1}(\omega) - \mathbf{G}^{-1}(\omega), \quad (\text{B1})$$

In order to be able to perform high precision calculation, it is necessary to be able to do exact subtraction of  $G_0^{-1}(\omega)$  and  $G^{-1}(\omega)$ . Direct subtraction of the calculated inverses of  $G_0(\omega)$  and  $G(\omega)$  at some point  $\omega$  is not a method of choice if we strive for high precision calculation. The reason lies in the finite precision arithmetics

in each computer. Details of this discussion will be given at the end of this section.

An alternative to the subtraction of the evaluated inverses of Green's functions is to subtract them as functions of the frequency and only then evaluate them in the frequency we are interested in. The difference with respect to the subtraction of already evaluated functions is that in this way we always subtract numbers of order one, whereas in the direct subtraction the subtracted numbers are sometimes large (in the vicinity of a pole) but close to each other. In this section we will focus only on the DIA case, i.e., local self-energy. Generalization to the non-local self-energies is straightforward.

If we mark the impurity site with index 1, then the self-energy on that site has a form

$$\text{Re}\Sigma_{11}(\omega) = [G_{0,11}(\omega)]^{-1} - [G_{11}(\omega)]^{-1} \quad (\text{B2})$$

where, in the case that each bath atom is connected only with the impurity site (starlike bath), the inverse of the free Green's function is obtained from the equations of

motion and reads

$$[\text{Re}G_{0,11}(\omega)]^{-1} = \omega + \mu - \epsilon_1 - \sum_{l=2}^{N_b} \frac{V_l^2}{\omega + \mu - \epsilon_l}, \quad (\text{B3})$$

where  $\epsilon_l$  is on-site energy,  $V_l$  is the hopping amplitude between bath sites and the impurity site,  $N_b$  is the number of atoms in the reference system and  $\mu$  is the chemical potential. From the Lehmann representation we know that the real part of the thermal one-particle Green's function on the real axis can be written in the form

$$\text{Re}G_{11}(\omega) = \sum_{i=1}^{N_G} \frac{C_i^{(1),G}}{\omega - \epsilon_i} \quad (\text{B4})$$

where  $C_i^{(1),G} > 0$  and  $\sum_i C_i^{(1),G} = 1$ ,  $N_G$  is a number of poles and  $\epsilon_i$ 's are poles of  $G_{11}(\omega)$ . The inverse of  $\text{Re}G_{11}(\omega)$  is then

$$[\text{Re}G_{11}(\omega)]^{-1} = C^{(0),G^{-1}} + \omega + \sum_{i=1}^{N_G-1} \frac{C_i^{(1),G^{-1}}}{\omega - \omega_i}, \quad (\text{B5})$$

where  $\omega_i$ 's are zeros of  $G$  (poles of  $G^{-1}$ ). Coefficients  $C_i^{(1),G^{-1}}$  are obtained if we equate the expression in Eq. (B5) with  $1/\text{Re}G_{11}(\omega)$ , where  $\text{Re}G_{11}(\omega)$  is given by Eq. (B4), and then calculate the limit  $\omega \rightarrow \omega_j$ . We get

$$C_j^{(1),G^{-1}} = \lim_{\omega \rightarrow \omega_j} \frac{\omega - \omega_j}{\sum_{i=1}^{N_G} \frac{C_i^{(1),G}}{\omega - \epsilon_i}} = \frac{-1}{\sum_{i=1}^{N_G} \frac{C_i^{(1),G}}{(\omega_j - \epsilon_i)^2}} \quad (\text{B6})$$

To have a value associated with  $C_i^{(0),G^{-1}}$ , we once again equate the expression in Eq. (B5) with  $1/\text{Re}G_{11}(\omega)$  from Eq. (B4) in any non-singular point  $\omega$ , but this time we use just calculated  $C_j^{(1),G^{-1}}$  coefficients. The procedure for the calculation of the derivative of  $\text{Re}G^{-1}$  with respect to some parameter of the reference system  $\lambda$  resembles the one used for the calculation of  $\text{Re}G^{-1}$ . From Eq. (B5) we see that  $\partial[\text{Re}G_{11}(\omega)]^{-1}/\partial\lambda$  can be written in the form

$$\frac{\partial[\text{Re}G_{11}(\omega)]^{-1}}{\partial\lambda} = \frac{-1}{[\text{Re}G_{11}(\omega)]^2} \frac{\partial\text{Re}G_{11}(\omega)}{\partial\lambda} \quad (\text{B7})$$

$$= C^{(0),dG^{-1}} + \sum_{i=1}^{N_G-1} \frac{C_i^{(1),dG^{-1}}}{\omega - \omega_i} + \sum_{i=1}^{N_G-1} \frac{C_i^{(2),dG^{-1}}}{(\omega - \omega_i)^2} \quad (\text{B8})$$

The coefficients  $C_i^{(1),dG^{-1}}$  and  $C_i^{(2),dG^{-1}}$  follow from

$$\begin{aligned} C_j^{(1),dG^{-1}} &= \lim_{\omega \rightarrow \omega_j} \frac{\partial}{\partial\omega} \left[ \frac{-(\omega - \omega_j)^2}{[\text{Re}G_{11}(\omega)]^2} \frac{\partial\text{Re}G_{11}(\omega)}{\partial\lambda} \right] \\ &= -2C_j^{(1),G^{-1}} \left( C^{(0),G^{-1}} + \omega_j + \sum_{\substack{i=1 \\ i \neq j}}^{N_G-1} \frac{C_i^{(1),G^{-1}}}{\omega_j - \omega_i} \right) \\ &\quad \times \frac{\partial\text{Re}G_{11}(\omega)}{\partial\lambda} \Big|_{\omega=\omega_j} - \left( C_j^{(1),G^{-1}} \right)^2 \frac{\partial^2\text{Re}G_{11}}{\partial\omega\partial\lambda} \Big|_{\omega=\omega_j} \quad (\text{B9}) \end{aligned}$$

$$\begin{aligned} C_j^{(2),dG^{-1}} &= \lim_{\omega \rightarrow \omega_j} \left[ (\omega - \omega_j)^2 \frac{-1}{[\text{Re}G_{11}(\omega)]^2} \frac{\partial\text{Re}G_{11}(\omega)}{\partial\lambda} \right] \\ &= - \left( C_j^{(1),G^{-1}} \right)^2 \left( \frac{\partial\text{Re}G_{11}(\omega)}{\partial\lambda} \right)_{\omega=\omega_j} \quad (\text{B10}) \end{aligned}$$

Unfortunately, the above equation for  $C^{(1),dG^{-1}}$  turned out to be numerically unstable, i.e., in practice we get only a few relevant digits correctly. There is another form in which we can write it and which is numerically stable. Taking the derivative of Eq. (B5) with respect to  $\lambda$ , we see that  $C_j^{(1),dG^{-1}} = \partial C_j^{(1),G^{-1}}/\partial\lambda$ . Now using Eq. (B6) we can show that  $C_j^{(1),dG^{-1}}$  equals to

$$- \left[ C_j^{(1),G^{-1}} \right]^2 \left( \frac{\partial^2\text{Re}G}{\partial\omega\partial\lambda} \Big|_{\omega_j} + \frac{\partial\omega_j}{\partial\lambda} \frac{\partial^2\text{Re}G}{\partial\omega^2} \Big|_{\omega_j} \right). \quad (\text{B11})$$

From the definition of  $\omega_j$ , i.e., zero of the Green's function, its derivative can be deduced and equals

$$\frac{\partial\omega_j}{\partial\lambda} = -C_j^{(1),G^{-1}} \frac{\partial\text{Re}G}{\partial\lambda} \Big|_{\omega_j}. \quad (\text{B12})$$

Coefficient  $C^{(0),dG^{-1}}$  then follows from Eq. (B8) with the coefficients Eq. (B11, B10) and Eq. (B7) if we equate them in an arbitrary non-singular point  $\omega$ . Having the inverses of the Green's functions and their derivative expressed as functions of frequency allows the representation of the self-energy with a sum of poles added to a constant term. Causality of  $\Sigma$  demands that each pole has a positive residue. As a consequence, the poles of  $[G_{0,11}(\omega)]^{-1}$  in Eq. (B4) are compensated by the poles of  $[G_{11}(\omega)]^{-1}$  from Eq. (B5). The final expression for the self-energy can thus be written in the form

$$\text{Re}\Sigma_{11}(\omega) = C^{(0),\Sigma} + \sum_{i=1}^{N_G-1} \frac{C_i^{(1),\Sigma}}{\omega - \omega_i}, \quad (\text{B13})$$

where  $C^{(0),\Sigma} = \mu - \epsilon_1 - C^{(0),G^{-1}}$  and  $C_i^{(1),\Sigma} = -\sum_l \delta_{\epsilon_l, \omega_i} V_l^2 - C_i^{(1),G^{-1}}$ . Analytic form of the derivative of the self-energy  $\frac{\partial\text{Re}\Sigma_{11}(\omega)}{\partial\lambda}$  is determined by Eqs. (B13, B3, B8)

$$C^{(0),d\Sigma} + \sum_{i=1}^{N_G-1} \frac{C_i^{(1),d\Sigma}}{\omega - \omega_i} + \sum_{i=1}^{N_G-1} \frac{C_i^{(2),d\Sigma}}{(\omega - \omega_i)^2} \quad (\text{B14})$$



TABLE II: Illustration of the degradation in precision by the evaluation of the self-energy for different frequencies using evaluated inverses of the Green's functions in Eq. B1 ( $2^{nd}$  column) in comparison with the result obtained from Eq. B13 ( $3^{rd}$  column). The calculation is done for the single impurity Anderson model with one bath site and for the parameters:  $U=4$ ,  $\mu = U/2$ ,  $\epsilon_c = 0$ ,  $T = 0.001$ ,  $\epsilon_2 = \mu$ ,  $V_2 = 0.5$ .

$\omega$	numeric	analytic
-1e-07	2.00278960194782	2.00000017777778
-5e-08	2.01115762927247	2.00000008888889
-1e-08	2.27893444799702	2.00000001777778
-4e-09	3.74339942335428	2.00000000711111
-2e-09	8.97438195502764	2.00000000355556
7.7e-23	1.6761776955e+15	2
2e-09	8.97277702135762	1.99999999644445
4e-09	3.74317856255584	1.99999999288889
1e-08	2.27895191107018	1.99999998222222
5e-08	2.01115782492434	1.99999991111111
1e-07	2.00278900765716	1.99999982222222

with

$$C^{(0),d\Sigma} = -\frac{\partial \epsilon_1}{\partial \lambda} - C^{(0),dG^{-1}}, \quad (B15)$$

$$C_i^{(1),d\Sigma} = -2 \sum_l \delta_{\epsilon_l, \omega_i} V_l \frac{\partial V_l}{\partial \lambda} - C_i^{(1),dG^{-1}}, \quad (B16)$$

$$C_i^{(2),d\Sigma} = - \sum_l \delta_{\epsilon_l, \omega_i} V_l^2 \frac{\partial \epsilon_l}{\partial \lambda} - C_i^{(2),dG^{-1}}. \quad (B17)$$

The derivative of the self-energy with respect to the frequency  $\omega$  is immediately evaluated from Eqs. (B3,B5) and reads

$$\frac{\partial \text{Re} \Sigma_{11}(\omega)}{\partial \omega} = - \sum_{i=1}^{N_G-1} \frac{C_i^{(1),G^{-1}} + \sum_l V_l^2 \delta_{\epsilon_l, \omega_i}}{(\omega - \omega_i)^2}. \quad (B18)$$

As commented at the beginning of this section, the above scheme is numerically more stable than the direct subtraction of the functions evaluated at a certain frequency  $\omega$ . This is illustrated in Table II. With a given precision of 8-byte floating point number (about 15 relevant digits) we see that direct evaluation gets the first relevant digit wrong already when the frequency is at a distance of  $\approx 10^{-8}$  from a spurious pole. Instead of having a finite value at  $\omega = 0$ , numerical calculation diverges. The non-existing divergence in the subtraction of the evaluated inverses of Green's functions has been removed in the step where we subtracted coefficients of  $G_0^{-1}$  and  $G^{-1}$ . As a result we have a small weight of the self-energy. If we had not nullified all small weights (small in comparison with the strongest pole), we would get very weak divergence in that point, but we know from the evaluation of the trace terms that weak poles give a small contribution to the grand potential. This allows us to nullify weights smaller than the precision determined primarily by the integration performed in the  $\text{Tr} \ln(-G_k)$  term. Aside from the loss of precision in the numerical algorithm, the appearance of the singularity at a point where the self-energy is supposed to be analytic might cause problems to the zero-searching algorithm.

\* Electronic address: kpozga@lusi.uni-sb.de

- <sup>1</sup> M. Potthoff, Eur. Phys. J. B **32**, 429 (2003)
- <sup>2</sup> A. Georges et al., Rev. Mod. Phys. **68**, 13 (1996)
- <sup>3</sup> J. M. Luttinger and J. C. Ward, Phys. Rev. **118**, 1417 (1960)
- <sup>4</sup> G. Baym, Phys. Rev. **127**, 1391 (1962)
- <sup>5</sup> P. W. Anderson, Phys. Rev. **115**, 2 (1959)
- <sup>6</sup> J. Kanamori, Prog. Theor. Phys. **30**, 275 (1963)
- <sup>7</sup> J. Hubbard, Proc. R. Soc. London, Ser. A **276**, 238 (1963)
- <sup>8</sup> M. Potthoff, Eur. Phys. J. B **36**, 335 (2003)
- <sup>9</sup> W. H. Press et al., *Numerical Recipes in C* (Cambridge

- University Press, New York, 1992)
- <sup>10</sup> Ning-Hua Tong, Shun-Qing Shen, and Fu-Cho Pu, Phys. Rev. B **64** 235109 (2001)
- <sup>11</sup> J. Joo and V. Oudovenko, Phys. Rev. B **64**, 193102 (2001)
- <sup>12</sup> R. Bulla, T. A. Costi, and D. Vollhardt, Phys. Rev. B **64**, 045103 (2001)
- <sup>13</sup> G. Beni and C. F. Coll, Phys. Rev. B **11**, 573 (1975)
- <sup>14</sup> R. Bulla, Phys. Rev. Lett. **83**, 136 (1999)
- <sup>15</sup> G. Baym, *Lectures on Quantum Mechanics* (W. A. Benjamin, Inc. Massachusetts, 1969)